 KSME Journal, Vol. 9, No. 3, pp. 312~322, 1995

Reduction of the Joint Clearance Effect for a Planar Flexible Mechanism

Y. S. Yoon,* J. S. Shim,* S. B. Lee* and K. D. Willmert**

(Received October 14, 1994)

When the operating speed of mechanical systems is increased, unpredictable dynamic problems are induced due to joint clearances and link elasticity. To solve these problems, quantitative prediction of the effects of joint clearance and link flexibility on the system is needed. This study has two principal objectives. The first is to develop a design method for eliminating the loss of contact at joints with clearance. The method utilizes three dimensionless parameters which govern the dynamic behavior at the instance when contact loss is predicted. These parameters are determined to maintain joint contacts throughout the operating cycle. The links in this mechanism are assumed to be rigid. The second objective of this study is to investigate the influence of the flexibility of the links. Using a finite element method, we found that link flexibility decreases the possibility of contact loss as well as the impact force at joints with clearance.

Key Words: Optimal Design, Flexible Mechanism, Clearance, Haines' Criterion

1. Introduction

During high speed motion of mechanical linkages sometimes unpredictable dynamic problems due to the link elasticity and the joint clearances occur. These problems result in degradation of the performance and life of the system. To solve these problems, the effects of joint clearance and link flexibility on the system performance are needed. It is also desirable to design mechanisms taking these effects into account.

Treatment of the complete problem(i.e., considering both the clearance and link flexibility) is complicated by the nonlinearities arising from joint clearances and large angular motion coupled with flexibility effects. Moreover, the inclusion of flexibility increases the dimensionality of the formulation. The resulting problem is beyond the analytical capabilities of most design establishments.

This study has two principal objectives. The first is to develop a design method for eliminating contact loss at that joint with clearance. The method is to introduce three dimensionless parameters that govern the dynamic behavior at the instant that contact loss is predicted, and to change these parameters to satisfy the condition that contact is maintained throughout the entire operating cycle. In this case, the links that are part of the mechanical system are assumed to be rigid. When the operating speed is increased, the effects of link elasticity become significant. That is the second objective of this study. The flexibility of the links is modeled by a finite element method. The study found that link flexibility has a direct influence upon whether contact is maintained or lost, i.e., link flexibility decreases the possibility of contact loss as well as the impact force at joints with clearance.

Early researchers analyzed one-dimensional impact problems due to clearances in the joints(Dubowsky, 1974) using repulsive coefficients and momentum conservation. Townsend(1975) and Miedema(1976) developed the pendulating model extending this one-dimensional model to two-dimensional rotational joints, where the surface of the joint bearing was

* KAIST, Taejon, Korea
** Clarkson Univ., Potsdam, N. Y., USA

assumed to be rigid. The motion after impact was again determined by the repulsive coefficient and momentum conservation.

Dubowsky(1971) introduced an impact pair using Kelvin-Voigt model(equivalent spring & damper model) that represents the bearing surface compliance. Advancing this model, Dubowsky and Gardener(1975) developed the IBM(Impact Beam Model) in which link flexibility is included, and found that link flexibility decreases the contact force at joints with clearance. Since the analysis of these problems requires a large amount of calculations, various methods to predict contact loss based on the analysis of zero-clearance mechanisms(so called nominal mechanisms) have been developed. The works of Earles and Wu(1975), Haines(1980), Fawcett and Burdess(1971) and Dubowsky et al.(1979) are examples.

Through experimental and analytical works, Earles and Wu proposed an empirical formula for prediction of the so called fly-past phenomena. According to their work, contact loss will occur at the instant when the bearing force becomes significantly reduced in magnitude R along with rapid change in direction b. Thus, the contact loss will occur when $|b/R|>1$. However, as Haines et al. pointed out, this formula is not of dimensionless form, thus losing its generality. Subsequently, various dimensionless formulas were proposed. Haines(1980) derived three dimensionless parameters for a general planar mechanism with one clearance joint and presented a design chart showing ranges of parameter values of which contact loss will occur. Dubowsky et al. (1979) proposed another dimensionless parameter named IPN(Impact Prediction Number) and noted that the occurrence of contact loss is very much dependent on the curvature of the joint path as well as on the driving speed and magnitude of the clearance.

These studies laid down simple design criteria for preventing the contact loss phenomena. Unfortunately, in spite of these successful studies, few design methods which systematically utilize the above mentioned criteria have been developed. Fawcett and Burdess(1972) considered bearing force loci to reduce the clearance effects. Three methods were suggested. They reported that except for the force-form-closure method(Earles and Kilicay, 1979), the use of balancing masses and balancing springs may require a trial and error approach to determine the correct configuration(Fawcett and Burdess, 1972). Haines(1980) come to the same conclusion.

Though not given in dimensionless form, Earles and Wu's criterion where the validity was shown through experiments by Earles and Kilicay(1971) and through simulation by Haines(1980), was used for the systematic design of mechanism to be free of contact loss by several researchers(Park and Kwak, 1987). Here the design methods use some balancing masses and springs, respectively.

In the present study, Haines' design chart and optimization techniques are used to design contact loss-free mechanisms. In this case, the objective function is a mass moment of inertia of additive balancing mass. The effects of link flexibility on the optimally designed mechanism are also considered.

2. Optimal Design of Mechanism with Clearance using Haines' Design Chart

Haines(1980) derived the equations that describe the conditions at a general idealized revolute joint with clearance, but with no hydrodynamic lubrication present. The equations are governed by three dimensionless parameters(h_1, h_2, h_3) that depend on the nominal motion, mass distribution and influence coefficients of the linkage in which the joint appears, as well as the clearance magnitude. The equations were solved numerically for a range of values for h_1, h_2, and h_3. The results enable the(h_1,h_2,h_3) space to be divided into two regions, one containing the values for which contact is lost at some time during the motion, the other in which contact is maintained throughout. The threshold surface between these two regions is in the form of a contour map, with h_1 and h_2 as polar coordinates, and contours joining equal values of h_3. In each case contact is lost on the inside of the contour and maintained on the outside.

In this paper, a systematic method is presented that moves the design point(on the chart) outwards on the contour by adding a balancing mass to the linkage. In this case, the mass moment of inertia of the balancing mass is chosen as the objective function to be minimized in the optimization. An offset slider crank mechanism is used as a numerical example.

2.1 Haines' design chart

Some assumptions are adopted to reduce the complexity of the problem to an extent that a general analysis becomes possible: that is, it is assumed that the joint can be extracted from the mechanism upon which the remainder of the mechanism is left undefined provided only that it is consistent with the assumptions. The key assumption of these ones is that whether contact is lost or maintained is determined by the conditions obtained at 'flypast': that is, moments in the cycle when the nominal bearing load vector undergoes a rapid change in direction and a simultaneous reduction in magnitude. The problem then can be reduced to describing the relative motion of the pin in the journal, as shown in Fig. 1, during the short interval containing the 'flypast' instant. The governing equation of motion of the system is a second order differential equation with three dimensionless parameters. These parameters are given by Haines(1980) as follows:

$$h_1 = R_u^* / (R_v^{*2/3} e^{2/3} M_0^{1/3})$$
$$h_2 = 2h$$
$$h_3 = e \tag{1}$$

Where R_u^* and R_v^* are u and v-directional joint contact forces respectively with dot denoting for the time derivatives. And M_0 is the generalized inertia, h and e are the angle of the principal direction and radius of the Mohr circle of the generalized inertia(Haines, 1980) respectively. Also the design chart, such as Fig. 2, can be constructed by searching the threshold surface(on this surface, the minimum joint contact force becomes zero) from the results of the governing equation for a range of values of h_1, h_2, and h_3.

For a given mechanism, the h-parameters can be calculated through the analysis of a nominal mechanism without clearances. The current state of the design can then be placed on the design chart. From this, one can be determined whether contact is lost or maintained. If the design point is inside of the contour corresponding to the current h_3, then contact is lost. In this case, some design change is needed(i.e., the current design point must be moved outside of the contour using an appropriate methods) to design a contact loss-free mechanism. Haines proposed three methods to avoid contact loss as follows:

(a) Use a spring element to increase the contact force between the pin and journal in a direction chosen so that the value of R_u^* is increased. This method has no effect on any of the variables in the

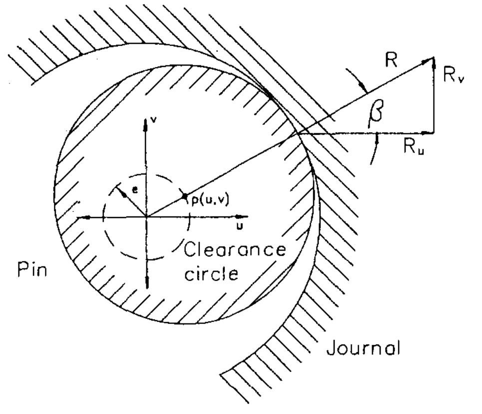

Fig. 1 Typical revolute joint with clearance

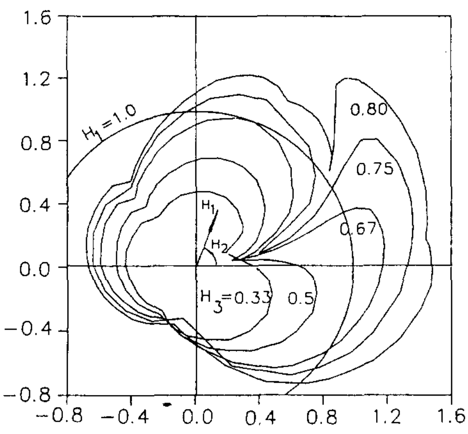

Fig. 2 Design chart

above analysis other than R_u^*, and hence h_1. The effect in the design chart is thus to move the design point radially outwards.

(b) Reduce the magnitude of the clearance, e. This method, like(a), implies change in h_1 with constant values for h_2 and h_3.

(c) Add a balancing mass to the linkage. Since this would affect all three dimensionless parameters, the selection of a suitable counterweight size and position for this purpose is a difficult problem.

Methods(a) and(b) have very practical restrictions. In case of(c), a systematic procedure is required to determine the balancing mass size and position. Haines has pointed out the difficulties in accomplishing this.

In the present study, a design method using an optimization technique, is proposed that determines the size and position of the balancing mass to avoid contact loss.

2.2 Formulation of optimal design problem

A general optimal design problem is to find the values of the design variables b at which an objective function

$$Y_0 = Y_0(\boldsymbol{b}) \tag{2}$$

is minimized under the constraints

$$\begin{aligned} Y_i &= Y_i(\boldsymbol{b}) = 0, \ i=1, \cdots, p \\ Y_i &= Y_i(\boldsymbol{b}) \leq 0, \ i=p+1, \cdots, q \end{aligned} \tag{3}$$

In this study, the mass moment of inertia of the balancing mass is selected as the objective function, with counterweight size(m) and position(a, b) as design variables(b_1, b_2, b_3). Also, a constraint condition is imposed so that the current design point is positioned under the threshold surface. This design problem can then be stated as follows:

minimize

$$Y_0 = b_1(b_2^2 + b_3^2) \tag{4}$$

subjected to

$$\begin{aligned} Y_1 &= h_3 - f(h_1, h_2) \leqq 0 \\ h_i &= h_i(b_1, b_2, b_3), \ i=1, 2, 3 \end{aligned} \tag{5}$$

where b_1, b_2, and b_3 are design variables and $f(h_1, h_2)$ is the threshold surface. To solve the optimal design problem, we need the sensitivities that represent the change of the functions Y_0 and Y_1 with respect to a change in design variables. In this case, the objective function is an explicit function of the design variable. Thus the sensitivity of the objective function can be calculated by the simple partial differentiation. But constraint function Y_1 is expressed in terms of h-parameters that are implicit functions of the design variables, where 'function' in this case does not mean a mathematically well-defined function, but rather a complex algorithm. Therefore, a finite difference differentiation technique was adopted to calculate sensitivities of the constraint function with respect to the design variables. Sensitivity vectors of objective function and constraint function are as follow:

$$\partial Y_0/\partial \boldsymbol{b} = [b_2^2 + b_3^2, 2b_1b_2, 2b_1b_3] = \boldsymbol{l}^{0T} \tag{6}$$

$$\begin{aligned} \partial Y_1/\partial \boldsymbol{b} &= [S\partial Y_1/\partial h_k \cdot \partial h_k/\partial b_1, \\ &\quad S\partial Y_1/\partial h_k \cdot \partial h_k/\partial b_2, S\partial Y_1/\partial h_k \cdot \partial h_k/\partial b_3] \\ &= [\partial Y_1/\partial h_1, \partial Y_1/\partial h_2, \partial Y_1/\partial h_3] \\ &\quad [\partial h_i/\partial b_j]_{3\times 3} \\ &\cong [\partial Y_1/\partial h_1, \partial Y_1/\partial h_2, \partial Y_1/\partial h_3] \\ &\quad [Dh_i/Db_j]_{3\times 3} \\ &= \boldsymbol{l}^T \quad i, j=1, 2, 3 \end{aligned} \tag{7}$$

where the subscript k is for summation from 1 to 3 and

$$\begin{aligned} &[\partial Y_1/\partial h_1, \partial Y_1/\partial h_2, \partial Y_1/\partial h_3] \\ &= [-\partial f/\partial h_1, -\partial f/\partial h_2, 1] \end{aligned} \tag{8}$$

And $\partial f/\partial h_i$, i=1, 2 are calculated by the following two steps:

Step 1. Divide the threshold surface into 4-node rectangular elements.

Step 2. The value of the function f and its derivatives with respect to h_1 and h_2 in elements are approximated by an isoparametric interpolation function.

2.3 Solution procedure of optimal design problem

With the design sensitivity information computed in the previous section, one can proceed to implement the optimization algorithm of choice. A gradient projection technique with constraint error correction(Haug and Arora, 1979) was used here for design optimization.

The gradient projection algorithm for design optimization in this particular case can be stated as follows :

Step 1 : Estimate an initial design $\boldsymbol{b}$.

Step 2 : Calculate the h-parameters constraint function value, and objective function value at the present design stage.

Step 3 : Check to determine whether the constraint function Y_1 is violated or not. If not violated, proceed with an unconstrained optimization step, followed by a return to step 2. If the constraint function Y_1 is violated, calculate the design sensitivity vector of Y_1 by the finite difference method :

$$\frac{\partial\psi_1}{\partial b_i} \cong \frac{\psi_1(\boldsymbol{b}', b_i+\Delta b_i)-\psi_1(\boldsymbol{b})}{\Delta b_i} \tag{9}$$

where $\boldsymbol{b}'$ is a vector that contains all of the design variables except b_i. The design sensitivity vector $\boldsymbol{I}$ is defined as

$$\boldsymbol{I}=\left[\frac{\partial\psi_1}{\partial b_1}, \frac{\partial\psi_1}{\partial b_2}, \frac{\partial\psi_1}{\partial b_3}\right]^T \tag{10}$$

Step 4 : The change in design $d\boldsymbol{b}$ is derived using Kuhn-Tucker necessary conditions applied to a linearized problem and is given as

$$\delta\boldsymbol{b}=-\eta\delta\boldsymbol{b}^1+\delta\boldsymbol{b}^2 \tag{11}$$

where

$$\eta=\frac{r\psi_o}{\frac{\partial\psi_o}{\partial \boldsymbol{b}}\delta\boldsymbol{b}^1} \tag{12}$$

in which r is the reduction ratio of cost function per iteration and $d\boldsymbol{b}^1$ and $d\boldsymbol{b}^2$ are given as

$$\begin{aligned}
&\delta\boldsymbol{b}^1=\boldsymbol{W}^{-1}\left[\frac{\partial\psi_o^T}{\partial\boldsymbol{b}}+\boldsymbol{I}\mu^1\right]\\
&\delta\boldsymbol{b}^2=-\boldsymbol{W}^{-1}\boldsymbol{I}\mu^2\\
&B\mu^1=-\boldsymbol{I}^T\boldsymbol{W}^{-1}\frac{\partial\psi_o^T}{\partial\boldsymbol{b}},\ B\mu^2=\psi_1\\
&B=\boldsymbol{I}^T\boldsymbol{W}^{-1}\boldsymbol{I}
\end{aligned} \tag{13}$$

Here, $\boldsymbol{W}$ is a positive definite weighting matrix to be selected by the designer. Put

$$\boldsymbol{b}^{(j+1)}=\boldsymbol{b}^{(j)}+\delta\boldsymbol{b} \tag{14}$$

Step 5 : The quantity

$$\|\delta\boldsymbol{b}^1\|=\sqrt{(\delta\boldsymbol{b}^{1T}\boldsymbol{W}\delta\boldsymbol{b}^1)} \tag{15}$$

is monitored. If all constraints are satisfied and $\|d\boldsymbol{b}^1\|$ is sufficiently small, terminate the process. Otherwise return to step 2 with $\boldsymbol{b}^{(j+1)}$ as the best available design.

3. Analysis of Flexible Mechanisms with Clearance

In Section 2, we discussed a design method for mechanisms with clearance, where the links and clearance joints are assumed to be rigid. But many researchers have found that the combination of elasticity in the links and joint clearances has a substantial effect on the dynamic behavior of the mechanism. Thus an investigation of the effects of link elasticity on the dynamics of the mechanism, designed using the method proposed at section 2, is needed.

In this section, a mathematical formulation of mechanism dynamics considering both link elasticity and connection clearance, using the finite element method(Bahat and Willmert, 1976), is presented.

3.1 Equations of motion

Figure 3 shows a general finite element i of link k. The displacement vector at any point A along the element measured from the origin of the fixed coordinate system($O: XY$) is given by :

$$\begin{aligned}S=&(X_1\cos(g)+Y_1\sin(g)+x+u_x)\boldsymbol{i}\\&+(Y_1\cos(g)-X_1\sin(g)+u_y)\boldsymbol{j}\end{aligned} \tag{16}$$

where (X_1, Y_1) is the rigid body position of end 1 of the element, x is the rigid body axial distance from end 1 to the general point A, g is the rigid body angle between the centerline of the link and

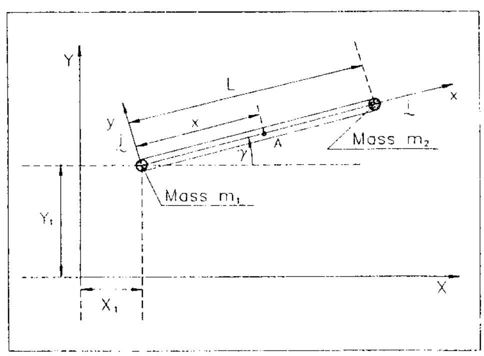

Fig. 3 Finite element model

the horizontal axis, and u_x and u_y are the axial and transverse deformations respectively of point. A due to elastic effects measured from the rigid body position. Differentiating this expression with respect to time results in the linear velocity, due to both rigid body and elastic effects, of any point in the element. It is noted that the unit vectors $\boldsymbol{i}$ and $\boldsymbol{j}$ are attached to a moving coordinate system and thus vary in direction with respect to time. The angular velocity of any differential line segment on the centerline of the element is given by:

$$\dot{\gamma}+\frac{d}{dt}\left(\frac{\partial u_y}{\partial x}\right) \tag{17}$$

The kinetic energy of the element is given by:

$$\begin{aligned} T=&\frac{1}{2}\int_0^L\Big(\rho A_x\dot{S}\cdot\dot{S}\\ &+I_x\Big(\dot{\gamma}+\frac{d}{dt}\Big(\frac{\partial u_y}{\partial x}\Big)\Big)^2\Big)dx\\ &+\frac{1}{2}(M_1\dot{S}\cdot\dot{S}\mid_{x=0}\\ &+M_2\dot{S}\cdot\dot{S}\mid_{x=L}) \end{aligned} \tag{18}$$

where ρ is the mass density, A_x and I_x are the cross-sectional area and mass moment of inertia respectively, and L is the length of the element. The second term on right side of the above kinetic energy expression is a rotary inertia term. The last two terms correspond to the kinetic energy of a slider or additive balancing mass.

The strain energy due to bending and axial deformation is:

$$U=\frac{1}{2}\int_0^L[EIu''^2_y+EA_xu'^2_x]dx \tag{19}$$

where E is the modulus of elasticity and

$$I=I_x/\rho \tag{20}$$

The external work associated with the element is:

$$W=\int_0^L[\tilde{\phi}_xu_x+\tilde{\phi}_yu_y+M_zu'_y]dx \tag{21}$$

where f_x, f_y, and M_z are externally applied distributed forces in the x and y directions and moment respectively. Concentrated forces and moments can be considered as well using the delta function to form equivalent distributed forces and moments.

Lagrangian function is then given by:

$$L=\sum_{k=1}^{S}\sum_{i=1}^{N_K}(T-U+W)_{ik} \tag{22}$$

where N_k is the total number of elements in the k-th member and s is the total number of members in the mechanism. Substituting the above energies and work expressions into Lagrangian function, it becomes a function of the unknown deformations u_x and u_y after the rigid body dynamics is determined. Both u_x and u_y are functions of position x along the elements and time. The usual approach in finite element work is then to approximate u_x and u_y.

In this study, u_x and u_y are approximated by 1st and 5th-order Hermite polynomials respectively; i.e.

$$\begin{aligned} u_x=&f_1(x)u_1(t)+f_5(x)u_5(t)\\ u_y=&f_2(x)u_2(t)+f_3(x)u_3(t)\\ &+f_4(x)u_4(t)+f_6(x)u_6(t)\\ &+f_7(x)u_7(t)+f_8(x)u_8(t) \end{aligned} \tag{23}$$

where

$$\begin{aligned} f_1(x)&=1-s\\ f_2(x)&=1-10s^3+15s^4-6s^5\\ f_3(x)&=L(s-6s^3+8s^4-3s^5)\\ f_4(x)&=L^2(s^2-3s^3+3s^4-s^5)/2\\ f_5(x)&=s\\ f_6(x)&=10s^3-15s^4+6s^5\\ f_7(x)&=L(-4s^3+7s^4-3s^5)\\ f_8(x)&=L^2(s^3-2s^4+s^5)/2\\ s&=x/L \end{aligned} \tag{24}$$

The terms u_1 and u_5 are the axial deformations at the left and right ends of the element respectively, and u_2 and u_6 are the transverse displacements at the ends, which are functions of time. u_3 and u_7 are the end rotations, while u_4 and u_8 are the end curvatures. Substituting the approximations of u_x and u_y into the Lagrangian results in a function of the generalized coordinates $u_1, \cdots, u_8$. These coordinates, for all of the elements and links, are not independent; i.e., they are related by the compatibility condition between adjacent elements. Following the general procedure of the finite element methods, however, we shall treat the element coordinate $u_1, \cdots, u_8$ as independent and derive the element equations of motion and then assemble the master equations later. The element equations are obtained by differentiating the Lagrangian with respect to element coordinates producing

$$\frac{d}{dt}\left(\frac{\partial L}{\partial \dot{u}_i}\right)-\frac{\partial L}{\partial u_i}=0,\ i=1,\ 8 \tag{25}$$

These equations result in the following ordinary differential equations :

$$\boldsymbol{m}\ddot{\boldsymbol{u}}+\boldsymbol{c}\dot{\boldsymbol{u}}+\boldsymbol{k}\boldsymbol{u}=\boldsymbol{f}(t) \tag{26}$$

where $\boldsymbol{m}$, $\boldsymbol{c}$, $\boldsymbol{k}$ depend on the rigid body motion of the mechanism as well as integrals of the products of the Hermite polynomials. $\boldsymbol{u}$ is a vector of element nodal coordinates :

$$\boldsymbol{u}=[u_1,\ u_2,\ u_3,\ u_4,\ u_5,\ u_6,\ u_7,\ u_8]^T \tag{27}$$

The forcing function $\boldsymbol{f}(t)$ also depends on the rigid body motion of the mechanism as well as the externally applied forces. The element nodal variables within the vector $\boldsymbol{u}$ are in terms of a moving coordinate system attached to each link. In order to assemble the elements and to equate corresponding coordinates, a transformation of element variables $\boldsymbol{u}$ is necessary. The usual approach is to transform all coordinates to the fixed global coordinate X and Y direction ; i.e., the transformation matrix $\boldsymbol{T}$ from $\boldsymbol{u}$ to $\boldsymbol{U}$ is

$$\boldsymbol{T}=\left[\begin{array}{cccc|cccc} \cos\gamma & \sin\gamma & 0 & 0 & & & & \\ -\sin\gamma & -\cos\gamma & 0 & 0 & & 0 & & \\ 0 & 0 & 1 & 0 & & & & \\ 0 & 0 & 0 & 1 & & & & \\ \hline & & & & \cos\gamma & \sin\gamma & 0 & 0 \\ & 0 & & & -\sin\gamma & -\cos\gamma & 0 & 0 \\ & & & & 0 & 0 & 1 & 0 \\ & & & & 0 & 0 & 0 & 1 \end{array}\right] \tag{28}$$

where $\boldsymbol{U}$ are the transformed element coordinates and g is rigid body rotation angle. Then the element differential equations becomes :

$$\boldsymbol{m}_G\ddot{\boldsymbol{U}}+\boldsymbol{c}_G\dot{\boldsymbol{U}}+\boldsymbol{k}_G\boldsymbol{U}=\boldsymbol{f}_G(t) \tag{29}$$

Once the element equations are calculated, the assembling process is done using the correlation between the transformed element nodal variable(U_i, $i=1$, 8) and the globally defined nodal variable(Q_i, $i=1$, n), where n is total degrees-of-freedom of the mechanism. The result will be a system of ordinary differential equations of the form :

$$\boldsymbol{M}\ddot{\boldsymbol{Q}}+\boldsymbol{C}\dot{\boldsymbol{Q}}+\boldsymbol{K}\boldsymbol{Q}=\boldsymbol{F} \tag{30}$$

The global mass, damping, and stiffness matrices are all functions of the rigid body motion of the mechanism and therefore the rigid body dynamics must be solved first. Once this is obtained, the above system of equations must be solved to determine the nodal displacement vector $\boldsymbol{Q}$. Since the system matrices($\boldsymbol{M}$, $\boldsymbol{C}$, $\boldsymbol{K}$) and forcing vector $\boldsymbol{F}$ are functions of rigid body motion and time, we need a differential equation solver in order to solve these equations. The second order differential equations of motion are reduced to first order form by a change of variables and solved by a predictor/corrector numerical integration algorithm(Shampine and Gordon, 1975).

3.2 Modeling of the planar revolute joint with clearance

Figure 4 shows a planar revolute joint which connects the links i and j, where the dotted lines represent the configuration of the nominal rigid mechanism. We define $\boldsymbol{R}$ as the position vector of the revolute joint of the nominal mechanism, U_i and U_j as the displacement vector of the joint axis point P of the nominal mechanism due to the link elasticity, and C_i and C_j as the contact points on the pin and the journal bearing, respectively. Therefore, the vectors $\boldsymbol{r}_i$ and $\boldsymbol{r}_j$, which are the position vectors of C_i and C_j in global coordinate system, and the velocity vector $\boldsymbol{v}_i$ and $\boldsymbol{v}_j$ of these points can be written as

$$\begin{aligned} \boldsymbol{r}_i&=\boldsymbol{R}+U_i-rd_iDp \\ \boldsymbol{r}_j&=\boldsymbol{R}+U_j-rd_jDp \\ \boldsymbol{v}_i&=\boldsymbol{R}+U_i-rd_iDp \\ \boldsymbol{v}_j&=\boldsymbol{R}+U_j-rd_jDp \end{aligned} \tag{31}$$

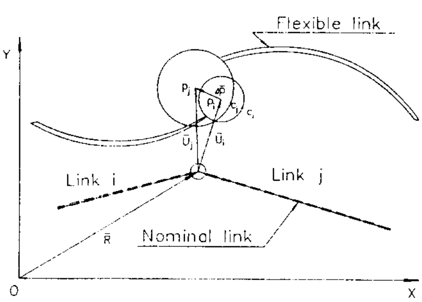

Fig. 4 Model of the planar revolute joint with clearance

where $\boldsymbol{Dp}$ is a unit vector along $\boldsymbol{Dp}(=\boldsymbol{U}_j-\boldsymbol{U}_i)$. The expressions rd_i and rd_j represent for the radii of the pin and journal respectively.

Once the relative position and velocity between the pin and journal are calculated, we can find the contact forces as

$$\boldsymbol{F}_i = k(|\boldsymbol{Dp}| - e)\boldsymbol{Dp} + c\{(\boldsymbol{U}_j - \boldsymbol{U}_i)$$
$$\boldsymbol{F}_j = -\boldsymbol{F}_i \qquad (32)$$

where k and c are the joint stiffness and damping coefficients respectively, and e is the magnitude of clearance between the pin and journal.

4. Results

An offset slider crank mechanism as shown Fig. 5 is considered. Its dimensional and inertial data are given in Table 1. We introduced a margin on the optimization constraint which specifies the threshold on Haines' design chart:

$$Y_1 = h_3 + M - f(h_1, h_2) \leq 0 \qquad (33)$$

where M is the design margin. Introducing a design margin means graphically lowering the threshold surface by m along the h_3-axis as shown in Fig. 6. We obtained the optimal design for three separate values of this margin, i.e., 0.0, 1.0 and 1.4. Results were obtained using a dynamic analysis of the slider crank mechanism with rigid links and clearance at the joint which connects the crank and the connecting rod. Figures 7, 8, 9, and 10 show the resulting joint contact forces at the clearance joint and corresponding numerical values are listed in Table 2. Figure 7 shows the joint contact force for the original mechanism, and Fig. 8 shows the results of the optimally designed mechanism with margin equal to 0.0.

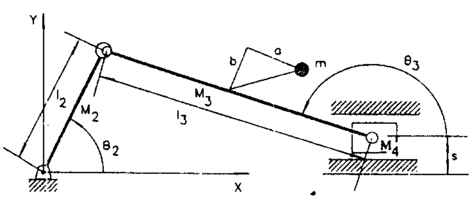

Fig. 5 An offset slider crank mechanism

Table 1 Properties of example mechanism

	Length(m)		Mass(Kg)	
	Symbol	Quantity	Symbol	Quantity
Crank	l_2	0.051	M_2	0.114
Coupler	l_3	0.152	M_3	0.341
Slider	-	-	M_4	0.341
Offset	s	0.051	-	-

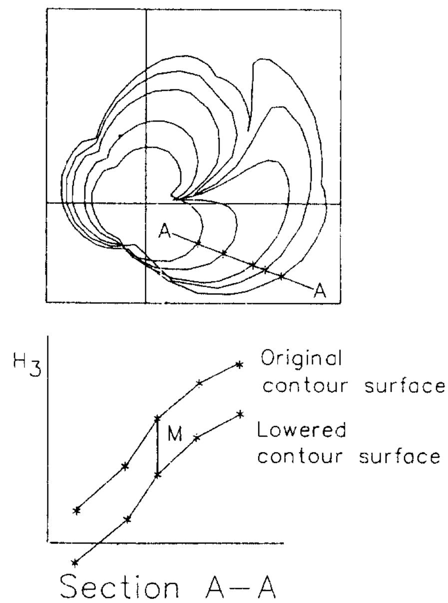

Fig. 6 Introduction of the design margin M

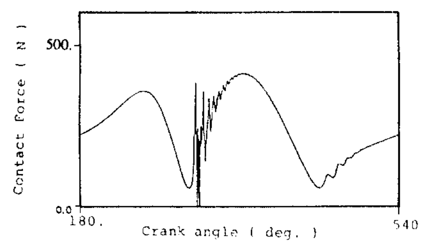

Fig. 7 Contact force of the original mechanism

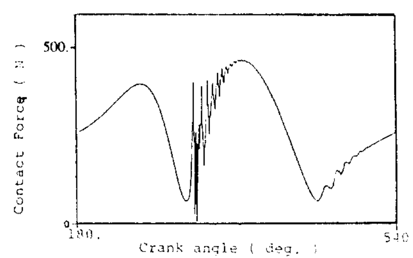

Fig. 8 Contact force of the mechanism that is optimally designed with margin 0.0

Table 2 Results of optimal design with constraint margins

Margin	Optimum values			
0.0	m	0.0980	h_1	1.15
	a	0.0004	h_2	−43.05
	b	0.0002	h_3	0.78
1.0	m	0.1500	h_1	2.39
	a	−0.0873	h_2	−41.30
	b	−0.0197	h_3	0.59
1.4	m	0.1605	h_1	3.09
	a	−0.1177	h_2	−35.60
	b	−0.0542	h_3	0.45

These results are nearly the same, because original mechanism is positioned nearly on the threshold surface of the design chart. Thus the optimally designed mechanism with margin zero is only slightly modified from the original mechanism.

The joint contact forces of the optimally designed mechanism with margins equal to 1.0 and 1.4 are shown as Figs. 9 and 10, respectively. In these cases, the contact forces are higher; thus the chance of contact loss at the clearance joint is diminished to nearly zero. Figure 9 also shows some fluctuation in the contact force which would influence the fatigue life of the joint surface. Therefore, the optimally designed mechanism with margin 1.4 is better because of less variation in the joint contact force as shown at Fig. 10.

The effects of link flexibility on contact loss at joints with clearance was studied using the theory developed in the previous section. These studies were performed through a comparison of results from four computational experiments. The analysis types for the computational experiment are classified as

(Ⅰ) Original Mechanism with rigid links
(Ⅱ) Original Mechanism with flexible links
(Ⅲ) Optimally designed mechanism with rigid links
(Ⅳ) Optimally designed mechanism with flexible links

Figures 7 and 11 show the contact forces at the joint between the crank and connecting rod in cases (Ⅰ) and (Ⅱ), respectively. From these results, we find that the flexibility of links has direct effect on the contact loss phenomenon, i.e., Fig. 7(with rigid links) shows some contact loss, but Fig. 11(with flexible links) shows continuous

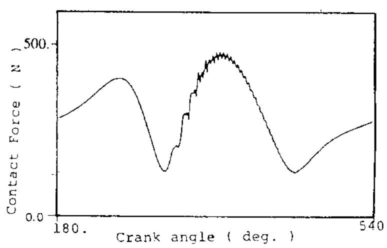

Fig. 9 Contact force of the mechanism that is optimally designed with margin 1.0

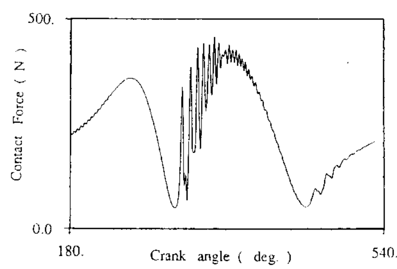

Fig. 11 Contact force of the original mechanism with flexible links

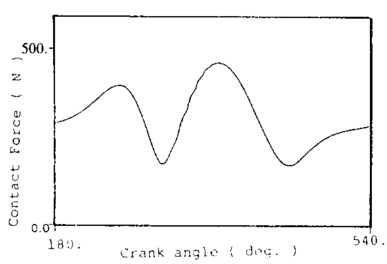

Fig. 10 Contact force of the mechanism that is optimally designed with margin 1.4

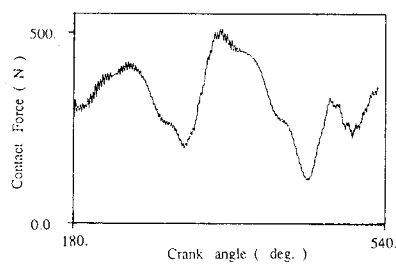

Fig. 12 Contact force of the optimally designed mechanism with flexible links(Margin 1.4)

contact. The stored strain energy excites a vibration as shown at Fig. 11, but this vibration may be diminished by applying the proper structural damping. Figures 10 and 12 show the contact forces for the optimally designed mechanisms with rigid and flexible links, respectively. As in the cases of (Ⅰ) and (Ⅱ), link flexibility has the effects of reducing the rapid change of the contact force.

5. Discussion

In general, it is known(Dubowsky and Gardener, 1975) that the flexibility of links reduces the impact forces at joints with clearance. But the effects on the contact loss itself is unknown, this is to say, whether the phenomenon which occurs in rigid link is maintained in the case of flexible links. This paper presents optimal design results, using Haines' design chart, for an offset slider crank mechanism with clearance and studies the effects of elasticity in links on the design. In designing a mechanism, positioning the design point on the threshold surface of Haines' design chart means that minimum contact force becomes zero. As a result, there is the possibility of contact loss if small disturbances occur. Once contact is lost, significant vibration may occur. That is why we introduced a design margin on the optimization constraint and obtained a satisfactory results with fairly smoothing joint contact forces additionally.

From the view point of contact loss phenomenon, link flexibility has definite effect on the behavior of mechanisms with clearance. The analysis considering link flexibility reveals less contact loss in the mechanism initially designed. However, when there is no contact loss as in the optimal design, link flexibility produces some member vibration along with more variation in contact force compared with the one ignoring link flexibility.

Acknowledgments

The authors are grateful to KOSEF for the support of this work through the grant #860308 and the National Science Foundation through grant #INI-8616036.

References

Bahat, B. M. and Willmert, K. D., 1976, "Finite Element Vibrational Analysis of Planar Mechanism," *Mechanism and Machine Theory*, Vol. 11, pp. 47～71.

Dubowsky, S. and Freudenstein, F., 1971, "Dynamic Analysis of Mechanical Systems with Clearances," Part Ⅰ & Ⅱ, *Trans ASME, J. Engng. Ind.*, Vol. 93, Series B, No. 1, pp. 305～316.

Dubowsky, S., 1974, "On Predicting the Dynamic Effects of Clearances in 1-D. Open-Loop Systems," *Trans. ASME, J. Engng. Ind.*, Vol. 93, Series B, No. 1, pp. 317～323.

Dubowsky, S. and Gardener, T. N., 1975, "Dynamic Interactions of Link Elasticity and Clearance Connections in Planar Mechanical Systems", *Trans. ASME, J. Engng. Ind.*, Vol. 97, No. 2, pp. 652～661.

Dubowsky, S., Prentice, J. M. and Valero, R. A., 1979, "On the Development of Criteria for the Prediction of Impact in the Design of High Speed Systems with Clearances," *Proc. 5th World Cong., IFToMM*, Montreal, Canada, pp. 968～971.

Earles, S. W. E. and Wu, C. L. S., 1975, "Predicting the Occurrence of Contact Loss and Impact at a Bearing from a Zero-clearance Analysis," *Proc. 4th World Cong., IFToMM*, Newcastle Upon Tyne, England, pp. 1013～1018.

Earles, S. W. E. and Kilicay, O., 1979, "Predicting Impact Conditions due to Bearing Clearances in Linkage Mechanisms," *Proc. 5th World Congress, IFToMM*, Montreal, Canada, pp. 1078～1081.

Fawcett, J. N. and Burdess, J. S., 1971, "Effects of Bearing Clearances in Four Bar Linkage," *Proc. 3rd World Cong.*, IFToMM, Kupari, Yugoslavia, pp. 111～126.

Fawcett, J. N. and Burdess, J. S., 1972, "Control of Clearance Effects in Linkages," *Engng. Mater. Des.*, Vol. 16, No. 1, pp. 26～27.

Haines, R. S., 1980, "A Theory of Contact Loss at Revolute Joints with Clearance," *J. Mech. Engng. Science*, Vol. 22, No. 3, pp. 129~136.

Haug, E. J. and Arora, J. S., 1979, *Applied Optimal Design*, John Wiley & Sons, pp. 77~88.

Miedema, B. and Mansour, W. M., 1976, "Mechanical Joints with Clearance: A Three Mode Model," *Trans. ASME, J. Engng Ind.*, pp. 1319~1323.

Park, C. B. and Kwak, B. M., 1987, "Counterweight Optimization for Reducing Dynamic Effects of Clearance at a Revolute Joint," *Mech. Mach. Theory*, Vol. 22, No. 6, pp. 549~556.

Shampine, L. F. and Gordon, M. K., 1975, *Computer Solution of Ordinary Differential Equations : The Initial Value Problem*, W. J. Freeman & Co., San Fransisco, Calif., pp. 41 ~52.

Townsend, M. A. and Mansour, W. M., 1974, "A Pendulating Model for Mechanisms with Clearances in the Revolutes," *J. Engng Ind.*, ASME Paper No. 74-DET-22.